5-2014

Investigating the Impact of Novel Iron Oxide Nanoparticles on Legionella pneumophila Biofilms and Trophic Interactions

Brennen Jenkins
Clemson University, brennej@g.clemson.edu

INVESTIGATING THE IMPACT OF NOVEL IRON OXIDE NANOPARTICLES ON *LEGIONELLA PNEUMOPHILA* BIOFILMS AND TROPHIC INTERACTIONS

A Thesis
Presented to
the Graduate School of
Clemson University

In Partial Fulfillment
of the Requirements for the Degree
Master of Science
Microbiology

---

by
Brennen Crenshaw Jenkins
May 2014

Accepted by:
Dr. Tamara McNealy, Committee Chair
Dr. J. Michael Henson
Dr. O. Thompson Mefford

ABSTRACT

Microbial biofilms serve as the base of food webs and are important for nutrient cycling in aquatic ecosystems. Nanoparticles (NPs) that enter into these aquatic systems have the potential to settle and become trapped within biofilms. As NPs become further integrated into consumer products, understanding their fate and effects on aquatic ecosystems is of paramount importance. Previous studies from our lab show that gold NPs induce dispersal of *Legionella pneumophila* biofilms. NPs with platinum and iron oxide core chemistries also lead to similar dispersal events, however, silver core NPs do not seem to induce these events due to NP aggregation. Chemical characteristics of NPs are also important in understanding the impact of NP contamination on trophic interactions. Gold NPs in biofilms altered bacterial interactions with amoebae but similarly-sized, highly stable iron oxide nanoparticles did not have the same impact. In this study we show that NPs become embedded within the extracellular polymeric substance (EPS) matrix of the biofilm. The EPS is composed of proteins, polysaccharides, and extracellular DNA (eDNA). We hypothesize that these NPs are potentially interacting with eDNA within the EPS causing destabilization that leads to biomass dispersal. We found that biofilms treated with DNase yielded a similar dispersion effect as treatment with NPs alone. Subsequent treatment with NPs after DNase (or DNase then NPs) showed no changes to biofilm dispersion after the initial treatment alone. eDNA is only one of several potential binding targets of NPs within the EPS. Future studies will investigate the mechanistic interactions of NPs with specific proteins and bacterial components that may also cause disruptive effects in biofilms.

ACKNOWLEDGMENTS

I would like to thank my advisor and mentor Dr. Tamara McNealy for all her guidance and knowledge during my time conducting research. Her patience and effectiveness as an instructor and mentor have made my time during graduate school productive and enjoyable. I truly appreciate having an advisor who not only serves as a guide on the journey through graduate school, but also someone who is a champion for their students. I would also like to thank my committee members, Dr. Mike Henson and Dr. O. Thompson Mefford for their invaluable assistance and advice during the course of this project. A special thanks to Dr. Terri Bruce for going above and beyond in helping me complete the imaging portion of my research. She has also served as an excellent source of knowledge and mentorship during my time at Clemson. I would also like to thank Rhonda Powell, the Clemson Light Imaging Facility, and Dr. Robin Schlicher of Leica Microsystems for their support and assistance in imaging. Very special thanks are due to my fellow graduate students Tara Raftery, Dr. Uma Mahajan, Andy Harmon, and Katie Jwanowski for their friendship and aid in running of the lab. I also want to acknowledge the help of David Limbaugh as well as the other undergraduates who assisted in keeping up with the lab. Finally, I am so grateful for my loving parents and boyfriend who have always encouraged my growth as a scientist and my pursuit of higher education.

TABLE OF CONTENTS

Page

Table of Contents (continued) Page

LIST OF TABLES

Table Page

LIST OF FIGURES

Figure Page

List of Figures (Continued)

Figure Page

INTRODUCTION

Nanoparticles: Importance and Behavior in Aquatic Environments

The field of nanotechnology has come to the forefront of materials science within the past decade and is quickly being integrated in a variety of fields including biology, chemistry, and physics. Nanomaterials are already found in a wide array of consumer goods and are predicted to be present in $3.1 trillion worth of these goods by 2015 (1). Nanomaterials are defined as a material with at least one dimension measuring between 1 and 100 nm and exhibit novel properties compared to their bulk counterparts. Engineered nanoparticles (NPs) in particular can be found in items such as sunscreen, cosmetics, athletic wear, and biosensors (Table 1).

Table 1. List of engineered nanomaterials found in various consumer products. Table from Suresh *et al.* 2013.

Nanomaterial	Consumer Product
Ag, CuO	Antimicrobial agent, medicinal devices, paints, plastics, clothing, household appliances
TiO_2, ZnO, CuO, Ni	Paints, ceramics, sunscreen, cosmetics, catalysts, batteries
CeO_2	Automobiles
Fe_3O_4	Medical devices, biochemical assays, water filters
Fe/Pt, Fe/Ni, SiO_2	Remediation of toxic elements, solar cells, electronics
Pt and Pd	Catalyst
Al_2O_3	Plastics, ceramics, polishing agent

NPs are known for their unique physico-chemical properties (such as high surface area to volume ratio) that enable use in a wide array of applications (2). While NPs are currently a hot topic in materials science, NPs themselves are nothing new. Naturally occurring NPs have existed for quite some time, being formed from geological

weathering, volcanic activity, or mineralization by organisms (2). Volcanic ash and fine sand are both examples of materials that exist as naturally occurring NPs. Many organisms have been gradually exposed to naturally occurring NPs over time and toxicity does occur, suggesting that engineered NPs are likely to cause toxicity (2).

Industrial products and waste potentially containing NPs ends up in waterways despite safeguards put in place by environmental agencies (3). The use and disposal of NP-containing products is not currently regulated by any one safety organization and there are no specific nanomaterials covered by the Toxic Substances Control Act or the Resource Conservation and Recovery Act (4). NPs are chemically identical to their bulk counterpart and are therefore not recognized as a new class of chemicals, even though

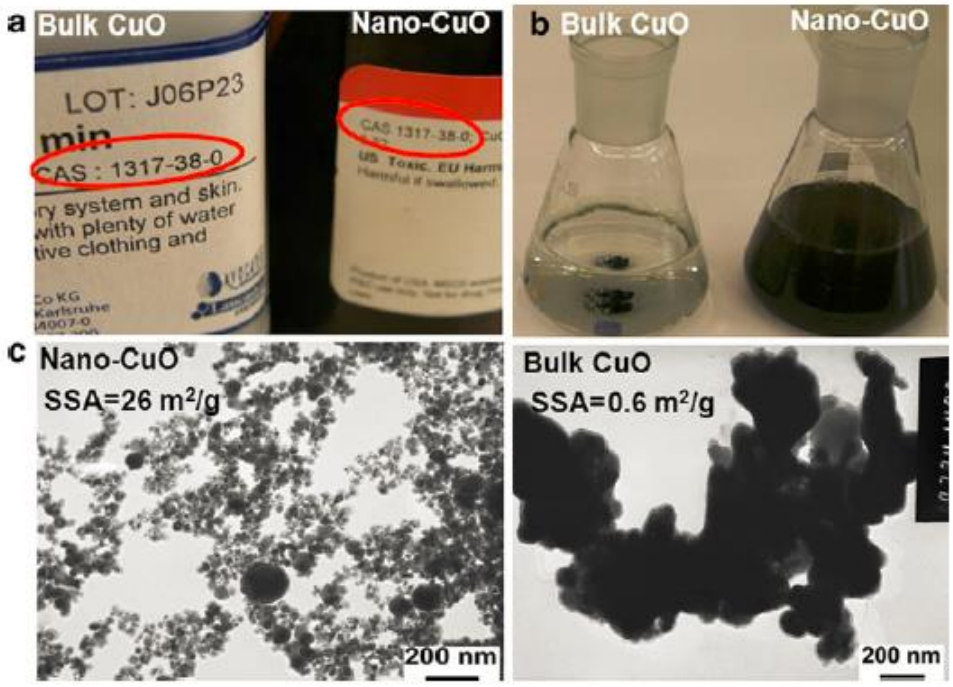

Figure 1. Differences in bulk versus nanoparticle chemicals. a) Labels of bulk versus nanosized CuO b) Suspensions of bulk and nanosized CuO c) TEM image of nanosized CuO versus bulk CuO. Figure from Bondarenko *et al.* 2013.

their properties are drastically different (Figure 1) (5).

NPs have the potential to become more stable in aquatic environments with dissolved organic matter and also have an increased surface area to volume ratio which leads to increased reactivity in these environments (5, 6). A better understanding of how these properties affect life in aquatic environments is important as the risk of entry into these systems becomes greater. Entry into aquatic environments can occur directly through migration into surface and ground waters, through wastewater effluents, or accidental spillage (7). Risk assessment for environmental contamination has been greatly overlooked when compared to protocols on manufacture and use of NPs. Before effects on aquatic organisms can be considered, it is necessary to understand the behavior and fate of NPs in the environment.

The environmental fate and transport of NPs is largely governed by particle size, surface and core chemistry, surface charge, and redox potential (8). Most colloids demonstrate aggregative behavior in the environment. NPs will often agglomerate to form particles greater than 1μm in diameter. The transport of these aggregated particles is mostly through sedimentation out of the water column. However, metal oxide NPs tend to sorb organic compounds in the environment resulting in nanoscale coatings that may prevent aggregation even in sea water. Other factors affecting the fate of NPs include environmental pH, ion concentration and the presence of other naturally occurring colloids (5-7). As more varied NP chemistries are constructed and utilized, the need to elucidate their effects on the environment becomes increasingly important to understand. To date, there are no comprehensive reports on physico-chemical behavior

influencing ecotoxicity of nanomaterials on aquatic microcosms in the natural environment. Overall, NP behavior is dynamic because of changing NP characteristics depending on environmental circumstance.

Nanoparticle Interaction with Aquatic Organisms

Many studies currently seek to understand NP toxicity in aquatic environments using sentinel animals to understand ecological consequences. A large majority of these studies are conducted using the aquatic invertebrates *Daphnia magna* and *Ceriodaphnia dubia*. Daphnids are an important part of aquatic ecosystems and serve as an energy link between primary producers and secondary consumers. Daphnids are essential in the degradation process of organic material and nutrient recycling and therefore serve as a model organism for studying ecotoxicity of engineered NPs. Acute toxicity of copper oxide (CuO), titanium dioxide (TiO_2), zinc oxide (ZnO), silver (Ag), and silicon dioxide (SiO_2) NPs has been observed in *D. magna* (9). Potential mechanisms of cellular toxicity include membrane disruption, production of reactive oxygen species (ROS) and harmful metal ions, DNA damage, and oxidation of proteins (7). AgNPs have been shown to be especially toxic with LC50 values for most organisms (from protozoa to crustaceans) falling below 10 mg/L. The toxic effect of AgNPs is explained by the generation of solubilized Ag^{+1} ions that can generate ROS. The toxicity of ZnONPs has been found to occur through a similar mechanism to AgNPs (5). A clear understanding of the toxicity mechanisms for different NPs is often challenging due to variations in testing conditions between laboratories, stability of NP in solution, NP surface coating and NP core chemistry.

Protozoa are another useful toxicological model organism for environmental research. *Tetrahymena thermophila* is a ciliated protozoa used in many nanoparticle toxicity studies analyzing cell proliferation, mortality, grazing capacity, and metabolic activity. ZnONPs have been shown to have a similar toxicity to *T. thermophila* as bulk ZnO (10). This similarity likely results from the equal concentrations of ionized zinc between NP and bulk form. AgNPs also demonstrate toxicity due to the production of silver ions that generate ROS leading to cell membrane damage (11). AgNPs, although not seen with ZnONPs in *Tetrahyamena*, often exhibit different harmful effects when compared to their bulk counterparts. CuONPs have been shown to be 10-20 times more toxic to *T. thermophila* than bulk CuO. Similar results were seen in algae and yeast with up to 60-fold differences in toxicity reported (10). *T. thermophila* is able to take up these NPs with food into the cell likely resulting in increased toxicity. CuONPs were found in aggregates attached to cell debris and within food vacuoles of *T. thermophila*. Titanium dioxide (TiO_2) NPs also induce acute toxicity in *T. thermophila* by interfering with cell growth likely similar to the mechanism observed with CuONPs. *T. thermophila* is also capable of taking up TiO_2NPs and storing them in food vacuoles until they are exocytosed as larger agglomerates (12). NPs can have a wide variety of interactions with varying organisms making it difficult to generalize issues of toxicity. A more complete understanding of how each type of organism can interact with NPs in the environment will enhance the knowledge of detrimental effects that can come from these interactions.

While many studies have been conducted understanding NP interactions with higher organisms, the level of the primary producer has not received as much attention.

It is of paramount importance to understand the effects of engineered NPs on bacteria, particularly bacterial biofilms. Most NPs undergo sedimentation upon entry into aquatic environments, making it likely that NPs will settle in ubiquitous microbial biofilms. Bacterial biofilms play an essential role in aquatic ecosystems; they are important for biogeochemical cycling and form the base of food webs (13). Disruption of these biofilms could have deleterious effects on entire ecosystems. Numerous studies have explored toxicity of engineered NPs on bacteria, focusing primarily on planktonic culture (11, 14-17). Most studies have used AgNPs that produce antibacterial properties through to the generation of ROS from dissolved silver (11, 15). Other NPs, such as TiO_2NPs and CuONPs have been shown to be bactericidal to *Escherichia coli* and *Pseudomonas putida*, respectively, at concentrations as low as 0.1 mg/L (18). Other engineered NPs have also been shown to disrupt cell division (ZnONPs), induce DNA damage (TiO_2NPs), impair growth (cadmium selenide NPs), and induce membrane disorganization (SiO_2NPs) (18). As with AgNPs, most of these NPs exhibit toxicity through the solubilization of metal ions. Other NPs, such as gold (Au) and platinum (Pt) NPs, are observed to be relatively non-toxic to bacteria, perhaps due to their poor solubility (18-21). While information on toxicity to planktonic bacteria is important, it is imperative to look at the preferred niche of most environmental bacteria, the biofilm (22).

Most studies concerning NP-biofilm interaction focus on antimicrobial action or methods to prevent biofilm formation (23-25). But, biofilms have also been shown to be a potential reservoir to trap and retain NPs. AgNPs and ZnONPs have been shown to become trapped and retained in *E. coli, P. aeruginosa,* and *Bacillus cereus* biofilms

covering porous surfaces (26-28). In one study, *E. coli* biofilm EPS was extracted and used to coat columns of porous media composed of crushed quartz sand. Using quartz crystal microbalance with dissipation monitoring (QCM-D), the deposition kinetics of ZnONPs were measured. Surfaces coated with biofilm EPS showed enhanced deposition of ZnONPs at varying fluid velocities. In another study by Xiao *et al.*, *P. aeruginosa* and *B. cereus* biofilms were grown on glass beads and subjected to fluid flow containing AgNPs coated with citrate and polyvinylpyrrolidone (PVP). NP concentration before entry into the column and after exiting the column was measured. AgNPs used in this study were found to be significantly retained by biofilm-coated columns. In another study, transmission electron microscopy revealed the presence of AgNPs embedded in *P. putida* biofilms (29). In the Fabrega *et al.* study AgNPs were shown embedded within the matrix and attached to bacterial cells (Figure 2). AgNP exposure induced a loss of biomass and increased biofilm sloughing. AuNPs, PtNPs, and Fe_3O_4 NPs also induce biomass loss in *L. pneumophila* biofilms at concentrations as low as 1μg/L (21). While toxicity of engineered NPs on bacteria is certainly an important aspect to consider when looking at NP contamination of aquatic environments, it is also important to understand the effects of NPs on microbial biofilms.

Figure 2. Transmission electron microscopy of *Pseudomonas putida* biofilms showing dark aggregates of AgNPs between bacterial cells and attached to bacterial cell surfaces. Figure from Fabrega *et al.* 2009.

EPS of Microbial Biofilms

Biofilms are complex communities of microorganisms found ubiquitously in aquatic environments. Microbial biofilms are essential to these environments as they are key players in biogeochemical and nutrient cycling. Microorganisms within a biofilm are held together by "glue" known as the biofilm matrix. This matrix is composed of mostly self-produced constituents known as extracellular polymeric substances (EPS). The EPS matrix forms a three-dimensional scaffold providing stability and maintaining adhesion to surfaces. This "glue" holds cells together allowing for cell-cell communication and retention of lysed cell components, transfer of genes, and nutrient distribution (30). EPS is generally composed of polysaccharides, proteins, and extracellular DNA (eDNA), yet the contribution of each biopolymer to biofilm integrity is not well understood (22, 30).

The amounts of these components can vary vastly between biofilms and are difficult to characterize in most biofilms. Polysaccharides play an important role in protection of the cells from antimicrobial agents and predators and are also important for maintaining a hydrated environment. Proteins like extracellular enzymes present in the EPS allow for degradation of macromolecules for nutrient acquisition and degradation of matrix components to allow release of cells from the biofilm. Lastly, eDNA enables bridging between cells, provides a means for transfer of genetic information, and aids in expansion of biofilms (22, 30). At a molecular level, NPs are most likely interacting with EPS material as it can make up to 90% of the biofilm. Understanding which components of the EPS NPs interact with and how will be important in determining the effects NPs will have on biofilms within aquatic environments.

eDNA plays an important role in formation and stability of several types of bacterial biofilms (31-34). *Pseudomonas aeruginosa* biofilms show specific self-organizing behavior of bacterial cells. eDNA in these biofilms has been shown to act as a traffic regulator that guide the flow of bacterial cells to the advancing edge of a growing biofilm. eDNA helps to align *P. aerugionsa* cells so that they function in a coordinated manner to promote biofilm expansion in a certain direction. The incorporation of DNase I in the media leads to traffic jams of cells which slowed biofilm expansion across semi-solid media (31). The mechanism of how eDNA may regulate traffic or what it may bind to on the bacteria has not yet been characterized. Gloag *et al.* proposed that the type IV pilus, which mediates twitching motility, may play a role in binding eDNA to interconnect cells within the biofilm. AuNPs in particular have been shown to tightly

bind DNA (35). One possibility is that NPs could interact with eDNA in the matrix, leading to destabilization and loss of biomass. AuNP-induced biomass loss could be due to binding of eDNA, leading to loss of eDNA connections that are stabilizing the biofilm. NPs may therefore be a useful tool to understand how matrix components play a role in stabilization of bacterial biofilms.

Effect of NPs on Bacteria-Grazer Interactions

Very few studies have been conducted to understand the effects of NPs on trophic interactions between biofilms and their protozoan predators. Protozoan grazing of bacteria provides protozoa with macronutrients and dietary metals as well as stimulating bacterial growth to create a rich microbial community (36). The interaction between bacteria and protozoa also plays an essential role in nutrient cycling. Grazing enhances the growth of bacterial populations responsible for biodegradation of contaminants but can also lead to potential biomagnification of toxic compounds (37).

Werlin *et al.* has shown that quantum dots (QDs) made of cadmium selenide accumulated in *P. aeruginosa* biofilms can be transferred and biomagnified in *T. thermophila* (36). Concentrations in the protozoan predator were found to be five times higher than in bacterial prey. QDs transferred to *T. thermophila* were toxic to protozoa and inhibited digestion in food vacuoles. Another study by Raftery *et al.* showed that AuNP-exposed *Legionella pneumophila* biofilms were less susceptible to grazing by the amoebae *Acathamoebae polyphaga* (38). Morphological changes to biofilms have been shown to increase grazing resistance by reducing a predator's ability to take in bacteria (39). If NP-induced morphological changes alone can disrupt normal predator-prey

interactions, there could be far-reaching implications for the integrity of the overall food web.

Environmental *Legionella*

Legionella are Gram-negative bacilli ubiquitously found in freshwater environments, both natural and man-made. The conditions for environmental survival of *Legionella* are relatively wide ranging. The bacteria can survive in temperatures of 5.0°C to 63°C and a pH range of 5.0-9.2 (40). Some species of *Legionella* survive in extremely acidic environments as low as pH 2.7. Most species of *Legionella* are strictly environmentally associated, but *Legionella pneumophila* can be potentially pathogenic to humans. *L. pneumophila* is the etiological agent of Legionnaire's disease, a form of pneumonia. *L. pneumophila* persists in environmental biofilms and grows optimally at temperatures between 32°C and 37°C. Inhalation of aerosolized bacteria from these biofilms, particularly biofilms in anthropogenic settings, can lead to disease outbreaks. *L. pneumophila* is able to parasitize free-living protozoans in the environment in order to persist in oligotrophic conditions. The ability of the bacteria to replicate within amoebae increases dissemination of the bacteria within the freshwater environment. The bacterium infects human alveolar macrophages in a similar manner to their environmental counterpart, the amoeba, resulting in human infection. The relationship between *L. pneumophila* and amoebae in the environment is well characterized, making it a good model system for analyzing trophic interactions between bacteria and protozoan grazers. By utilizing this model, we are able to investigate the impact NP contamination may have on interactions between biofilms and protozoan grazers.

L. pneumophila can also take advantage of encysted amoebae and be protected from harsh chemicals or heat. Amoebae are able to go into a dormant cyst form by forming into a tight ball and secreting a protective membrane. In this form, amoebae are resistant to harsh environmental conditions and chemicals. When conditions become favorable, the amoebae leave the cyst form. Intracellular bacteria can be protected in vacuoles within the amoebae until the protozoa decyst, allowing the bacteria to escape biocidal chemical treatment (40). This mechanism of chemical treatment evasion is particularly a problem in anthropogenic settings such as cooling towers. Biofilm growth in piping can reduce heat transfer and fluid flow in cooling towers. One commercial method of eradicating these biofilms is through the use of harsh chemical biocides. *L. pneumophila* are protected within encysted amoebae from biocide treatment and go on to colonize new biofilms once the treatment has ceased. This leads to regrowth of biofilms that once again require biocide treatment.

The *L. pneumophila* biofilm has been the focus of many studies concerned with preventing disease outbreaks, however, less is known about the specific constituents that comprise these biofilms. Understanding components that play a role in biofilm stabilization is important for disease prevention and biofilm eradication, especially in man-made settings. *L. pneumophila* exist as part of a microbial community, rich in a variety of different prokaryotes and eukaryotes. As previously described, *L. pneumophila* is able to use amoebae as a vehicle for replication. NP contamination could potentially have a deleterious effect on this relationship and understanding NP impact on invasion and replication of the bacteria in amoebae is an important part of this study. It has been

shown that bacterial replication within amoebae is an important factor in the bacterium's ability to colonize new biofilms. Bacteria grown in amoebae were shown to produce aggregated microcolonies with excess production of polysaccharides when compared to biofilm colonization by medium grown bacteria (41). This could be a protective mechanism in which bacteria leaving the nutrient rich vacuole of amoebae are better suited to form a thick biofilm in oligotrophic conditions. Understanding how these aggregated microcolonies are formed could yield more information on how biofilms form at a molecular level. Autoaggregation of the bacterium has recently been shown to be facilitated by the *Legionella* collagen-like protein (Lcl). Autoaggregation is also shown to be correlated with strength of biofilm production (42). Lcl has been shown to be crucial for biofilm formation in *L. pneumophila* (43). Mutants lacking Lcl are deficient in autoaggregation and have a reduced ability to disseminate in man-made water systems. Ion concentration is another important dictator of how *Legionella* biofilms form in the environment likely connected to induction of bacterial autoaggregation that involves Lcl.

Presence of certain ions has been shown to enhance or inhibit attachment of the bacterium during the initial stages of biofilm formation. Calcium, magnesium, and zinc have been shown to induce autoaggregation, and therefore increase the bacteria's ability to colonize new biofilms (42). Calcium and magnesium facilitate attachment of *L. pneumophila* to surfaces while copper tends to decreases the bacterium's ability to attach (44). In anthropogenic settings, flow forces appear to play a role in *L. pneumophila* biofilm formation. Stagnation of water flow helps encourage attachment of the bacterium

to abiotic surfaces, while turbulent flow can help maintain already established *L. pneumophila* biofilms (45).

Very little is known about the role of EPS components in *Legionella* biofilm stability and maturation, thus elucidation of the molecular interactions NPs have with particular EPS components of the *L. pneumophila* biofilm will help reveal new information about NP-biofilm interactions. These interactions will become more important to understand as NPs become more commonplace. The purpose of this study is to investigate specific mechanisms of NP-mediated biofilm dispersion. The goal was to characterize the interaction of NPs with eDNA associated with *L. pneumophila* biofilms and determine if eDNA is an essential component for stabilization of these biofilms. Our hypothesis is that highly stable Fe_3O_4 NPs mediate biofilm dispersion through the same (or related) mechanisms as AuNP-mediated biofilm dispersion seen previously in work from our lab. Similar loss of biomass has been seen when *L. pneumophila* biofilms were exposed to both types of NPs. AuNPs disrupted trophic interactions between bacteria and amoebae therefore we predicted that Fe_3O_4 NPs would have a similar effect on trophic interactions if the mechanisms of biofilm dispersal are the same. This study seeks to characterize NP-eDNA interactions, eDNA's involvement in biofilm stabilization, and the role of NP chemistry in disruption of trophic interactions.

MATERIALS AND METHODS

Organisms and Media

L. pneumophila Philadelphia 1 (ATCC 33152) was cultured on buffered charcoal yeast extract (BCYE) agar at 26ºC for 3 days. Bacteria from an agar plate were resuspended in ACES (*N*-(2-acetamido)-2-aminoethanesulfonic acid)-buffered yeast extract (AYE; pH=6.9) broth to appropriate optical densities (OD) for the experiments.

Axenically grown cultures of *Acanthamoebae polyphaga* (ATCC 30461) were grown independently in 25 mL tissue culture flasks in tryptic soy broth (TSB) at 23°C.

Moderately hard water (MHW; 18 MΩ and produced with reagent grade salts, hardness = 80 mg $CaCO_3$/L, alkalinity = 60 mg $CaCO_3$/L, pH = 7.7) was used as the exposure media in all biofilm exposures.

Nanoparticle Synthesis

Spherical, citrate-capped 18nm AuNPs were synthesized according to Gole and Murphy (46). AuNPs were synthesized and stored in ultrapure water at room temperature (UPW; 18 MΩ). Untagged, poly(ethylene oxide) 3,4 dihyroxy-L-phenylalanine (nitroDOPA) Fe_3O_4 NPs were synthesized as previously described (38, 47). Cy5.5 modified Fe_3O_4 NPs were synthesized by Dr. Roland Stone. First 7.2 nm Fe_3O_4 NPs were modified with a multidentate heterobifunctional polyethylene oxide (PEO) that had an alkyne on one end and a nitroDOPA group on the other end to anchor to the iron oxide nanoparticles, using a modified synthetic procedure from Na *et al.* (48). Cy5.5 was then 'clicked' onto the surface using copper(II) sulfate and sodium ascorbate to create a copper (I) catalyst *in situ* and dialyzed for 3 days to remove any free Cy5.5 and copper catalyst.

Nanoparticle Characterization

AuNPs were characterized by dynamic light scattering (DLS) and zeta potential (Malvern Zetasizer Nano ZS) in the ultrapure water (UPW) stock solution. DLS was performed using a Wyatt Dawn Heleos™ with ASTRA® 6 software for data collection. DLS measures the hydrodynamic diameter of the particles in solution by measuring variations in scattered light intensity due to Brownian motion. Analysis of these intensity fluctuations determines particle size using the Stokes-Einstein relationship. The concentration of AuNP stock was 30,471 μg/L as determined by inductively coupled plasma mass spectroscopy (ICP-MS). Untagged Fe_3O_4 NPs were also characterized in UPW stock solution using DLS and zeta potential (Malvern Zetasizer Nano ZS). Zeta potential is measured by using the electric double layer formed outside of a particle in liquid suspension. This potential is calculated by measuring the velocity of particles as they move through a laser beam. Core size of Fe_3O_4 NPs was determined by transmission electron microscopy (TEM) as previously described (38, 47). Fe_3O_4 NPs stock concentration was 500,000 μg/L of Fe as determined by ICP. Fluorescence of Cy5.5 tagged Fe_3O_4NPs was confirmed by photoluminescence analysis.

Biofilm Establishment

L. pneumophila biofilms were formed by re-suspending bacteria from a 3-day-old BCYE agar plate in AYE to an OD_{600}= 0.6. Biofilms were grown on glass slides placed within glass petri dishes or coverslips placed within plastic well plates. Re-suspended bacteria were added to these dishes or well plates in 10% AYE solution for 24 hours to promote initial attachment of the bacteria at 26°C. After 24 hours incubation, the supernatant was

removed and replaced with 100% AYE to allow for biofilm growth. The biofilms were then incubated for four additional days at 26°C. On day five, the *L. pneumophila* biofilm is considered mature. Mature biofilms to be used in NP exposure experiments were washed once with UPW. The medium was then replaced with either MHW or MHW plus NPs. NPs were added at a concentration of 1 or 100 μg/L for these experiments. After a further 48 hours of incubation, biofilms were once again washed twice with UPW. Slides were then aseptically removed, air dried, and fixed in methanol for 10 minutes. After fixation, biofilms were stained with 3 μM Syto11 nucleic acid stain (Invitrogen) for 30 minutes. Slides were then rinsed with UPW and coverslips were mounted using a 50/50 v/v solution of glycerol:phosphate buffered saline (1X PBS).

Amoebae Viability and Replication

Amoebae viability and replication experiments were conducted as previously described (38). *A. polyphaga* trophozoites were collected from tissue culture flasks and counted using a trypan blue assay. Viability and replication assays were conducted in both TSB and MHW. For viability assessment in TSB, flasks with approximately 80% confluency of amoebae received either TSB only or TSB with 100 ug/L Fe_3O_4 NPs. Flasks were statically incubated for 48 hours at 23°C. Amoebae were then collected and counted using the trypan blue assay. Three independent replicates were performed.

For assessment of viability and replication in MHW, amoebae were collected from confluent flasks then resuspended into sterile MHW and seeded into 25 cm^3 flasks. Treated amoebae received 100 μg/L Fe_3O_4 NPs and were incubated for 24 hours, 48 hours, or 72 hours. Controls received sterile MHW only. At each time point, amoebae

were collected and counted using a trypan blue assay. Percentage of live (trophozoites and cysts) and dead amoebae were determined. Following this assessment, a 1:100 dilution of amoebae from one flask at each time point was inoculated into fresh TSB to determine effects of NP exposure on excystment and recovery. Amoebae were counted using the trypan blue assay every 12 hours for 48 hours after inoculation into fresh TSB. Three independent replicates were performed.

Amoebae-*Legionella* Interaction Assays

Planktonic Bacteria Infection Assay

Infection assays using planktonic *Legionella* were conducted as previously described (38, 49). Briefly, $1x10^6$ *A. polyphaga* were seeded into six-well plates and incubated overnight at room temperature. *L. pneumophila* was added at a multiplicity of infection of 100:1 (bacteria to amoebae) either alone, simultaneously with 100µg/L Fe_3O_4 NPs, or after incubating the bacteria overnight with 100 ug/L Fe_3O_4 NPs. Bacterial invasion was assessed at 2 hours and bacterial replication at 48 hours. Amoebae were collected, lysed and plated for bacterial colony-forming unit determination at each time point. Three independent replicates were performed.

Amoebae Grazing Assay

Grazing assays were conducted as previously described (38). Biofilms were established in 10% AYE in sterile petri dishes on glass slides. On day five, Fe_3O_4 NPs added at a concentration of 1 µg/L in 20ml sterile MHW to treatment biofilms while controls received 20 ml of sterile MHW. Previous studies have shown that a 1 µg/L concentration of both NPs leads to significant dispersal of the biofilm (21). 48h after the NP exposure,

biofilms were washed and $1x10^6$ amoebae were added to each biofilm. Biofilm samples included the following: (1) *L. pneumophila* only, (2) *L. pneumophila* + 10^6 *A. polyphaga*, (3) *L. pneumophila/*NP exposed, (4) *L. pneumophila/*NP exposed + 10^6 *A. polyphaga.* After 48 hours, amoebae were collected from each biofilm as previously described (38). Amoebae survival was determined using a trypan blue assay. The slides were then removed and air dried before fixation in methanol for surface area analysis. Slides were then stained with 0.1% crystal violet, imaged (three fields per slide, 60x magnification, Nikon TE2000 microscope), and subsequently analyzed via COMSTAT to determine the surface area of the biofilm. Five independent replicates were conducted.

Analysis of Dispersed Biofilm

Biofilms were grown as previously stated on glass slides in sterile glass petri dishes. On day five, AYE was replaced with MHW alone or MHW plus Fe_3O_4 NP treatment. Biofilms were treated at a concentration of 1 μg/L of each NP for 48 hours at 26°C. After 48 hour incubation, biofilm supernatant was removed and collected in separate conical tubes for each treatment. Biofilms were washed twice with UPW and these washes were added to the collected supernatant. The collected supernatant with additional washes was centrifuged at 4,000 rpm for 20 minutes at 23°C. The pellet was re-suspended in 1 mL of UPW and serial dilutions were plated on BCYE to determine the number of viable cells released from the biofilm in CFU/mL.

Microscopy: Nanoparticle-Biofilm Interaction

CytoViva Hyperspectral Microscopy

Mature *L. pneumophila* biofilms were established in sterile petri dishes on glass slides as described above (20). Biofilms were washed twice with UPW then incubated at 26°C for 48h in MHW or MHW + 100μg/L AuNPs or Fe_3O_4 NPs. Biofilms were washed twice again with UPW, then fixed in methanol. A control slide of only AuNPs and only Fe_3O_4 NPs was made by allowing a drop of nanoparticles to dry onto a glass slide. Immersion oil was added to all slides, followed by placement of a cover slip. A CytoViva (CytoViva, Auburn, AL) hyperspectral imaging system was used to examine the slides. This system employs enhanced dark field illumination to produce light scattering from NPs and cells. As NPs are generally smaller than the wavelength of light and have tightly packed atoms, they tend to scatter light much more than their surrounding environment. Utilizing a spectrophotometer, the spectral signature from the light scattered by the NPs can be collected and used to build a spectral library, which can be subsequently used to identify the presence of the NPs in other samples. A spectral library file was built using a slide of AuNPs only or Fe_3O_4 NPs only. Approximately 20 unique spectra were collected for each NP library. A spectral angle mapping (SAM) classification was carried out on both control and treated biofilms with a default tolerance of 0.100 in matching spectra for the NPs. Pixels that matched the spectral profile of an NP are colored red in images.

Leica Ground State Depletion Microscopy with Cy5.5 - Fe_3O_4 NPs

L. pneumophila biofilms were established in six well plates on sterile glass coverslips in 10% AYE. After five days, biofilms were gently washed once with 1 mL UPW and exposed to 1µg/L Cy5.5-tagged Fe_3O_4NPs in MHW. After 48 hours, biofilms were washed with 1X PBS then allowed to air dry. Biofilms were fixed in 4% paraformaldehyde, gently washed with 1X PBS, and then stained with Syto11 nucleic acid stain (Invitrogen). Mowiol® mounting medium was added to a depression slide and the dried coverslip was carefully placed over this filled depression, biofilm side down. The edges of the coverslip were sealed with Twinsil® and allowed to harden for 5-10 minutes. The biofilms were imaged on a Leica SR GSD 3D, Super Resolution Ground State Depletion 3D Microscope (Leica Microsystems, Buffalo Grove, IL) using a 160X TIRF objective with a cylindrical lens (Leica HCX PL APO 160X / 1.43 NA, oil immersion). Ground state depletion microscopy (GSD) relies on the fact that certain fluorophores can be driven into a "dark" triplet state. In GSD, a laser is used to first drive the fluorophores into the triplet state. Fluorophores return from the triplet state at different times and emit light as they return to the ground state. This results in a "blinking" phenomenon allowing neighboring fluorophores, which would not normally be resolvable from one to another, to be seen individually. The coordinates of the resulting individual points of light are used to construct the final super resolution image. This technique results in resolutions of down to 20 nm laterally and 50 nm axially.

AuNP-DNA Binding Analysis

The plasmid pBC KS (Stratagene) was used to assess DNA binding of AuNPs. Purified plasmid was collected by a Wizard® Plus Midipreps DNA Purification System

(Promega) with a final concentration of 83 ng/μL pDNA stock was stored at -20 °C. Isolated pDNA was added directly to the MHW at a normalized 1% v/v (i.e. 15 μL pDNA in 1500 μL total volume). NPs were then added at 6.5 mg/L final NP concentration. The 1 μg/L concentration used in biofilm-nanoparticle assay was below the detection limit of the Zetasizer used in this analysis. The 1.5 mL sample was immediately aliquoted into a zeta cell and placed in the Zetasizer for the time zero measurement (t=0). Interactions were assessed at 0, 30 minutes, 24h, 48h, and 72h. All measurements reported represent triplicate independent samples.

Biofilm Interaction Analysis

NP-DNAse Assay

Interactive effects from NPs, DNase, or a combination of the two on biofilms were assessed. Mature *L. pneumophila* biofilms were established as described above. Control biofilms were exposed to MHW, MHW + 1 μg/L AuNPs, or MHW + 1 μg/L Fe_3O_4 NPs for 48h. Biofilms were then washed twice and half subsequently treated with 1 U/μL RQ1 DNase (Promega) in MHW for two hours with gentle shaking of the petri dish every 30 minutes to ensure mixing. Biofilms were fixed in methanol and stained with nucleic acid stain Syto11 (Invitrogen) for analysis. Confocal microscopy images of three fields / biofilm were acquired at 60x magnification on a Nikon Ti Eclipse Confocal Microscope. Bio-volume, thickness, and roughness were quantified using COMSTAT image analysis software through MATLAB. Three independent replicates were performed.

DNAse-NP Assay

Biofilms were established and treated as above, except that half of the biofilm slides were subjected to 1 U/μL RQ1 DNase in MHW for two hours first. Control biofilms that did not receive DNase treatment received MHW only. After DNase treatment, biofilms were washed and exposed to either MHW only, or one of the two NP treatments for 48 hours. Biofilms were then washed, fixed, stained and imaged as described above. Bio-volume, thickness, and roughness were quantified using COMSTAT image analysis software through MATLAB. Three independent replicates were performed.

Image Analysis

Image analysis using the program COMSTAT was conducted as previously described (38, 50). For surface area analysis, images taken were in a two-dimensional plane of view at the surface of the biofilm. Surface area was quantified as the amount of biomass occupying the plane of view at the surface of the biofilm. For bio-volume analysis, images were taken and analyzed as three-dimensional confocal stacks. Bio-volume was quantified as the amount of biomass occupying each plane of view of the entire confocal stack. Thickness of the biofilm was also determined as the average height of the entire biofilm. Roughness coefficient was also determined from COMSTAT analysis.

Statistical Analysis

Statistical analyses were conducted as previously described (38). A Wilcoxon rank-sum test was used to compare percentage of live and encysted amoebae for NP treatment of viability experiments. A Student's *t* test was used to compare the growth kinetics of amoebae after NP exposure compared to the control at each time point. A one-way analysis of variance (ANOVA) was used for the planktonic-phase interaction assays, to

compare the surface area and to compare amoebae survival after NP treatment. When significant differences were found, Fisher's least significant difference was used to analyze which treatments significantly differed from the others. A significance level of $p<0.05$ was used for all tests, and statistically significant differences are denoted with asterisks on graphs.

RESULTS

Nanoparticle Characterization

Characterization of 20 nm synthesized AuNPs was conducted as previously described using DLS to analyze hydrodynamic diameter in solution (20). DLS demonstrated AuNPs of the expected size, 25.28 nm. Characterization of Fe_3O_4 NPs was conducted using DLS and zeta potential to determine hydrodynamic diameter and stability in solution, respectively (38, 47). The Fe_3O_4 NPs had a z-average diameter of 73.0nm by DLS and a core size of 7.4nm by TEM; zeta potential was found to be about -12.2 mV. The z-average diameter from DLS measurements are higher due to the large PEG polymer complex attached to the Fe_3O_4 core. Cy5.5 tagged particles were excited at 665 nm and a photoluminescence response was observed at 701 nm. Cy5.5 tagged Fe_3O_4 NPs response at 701 nm is expected for this dye.

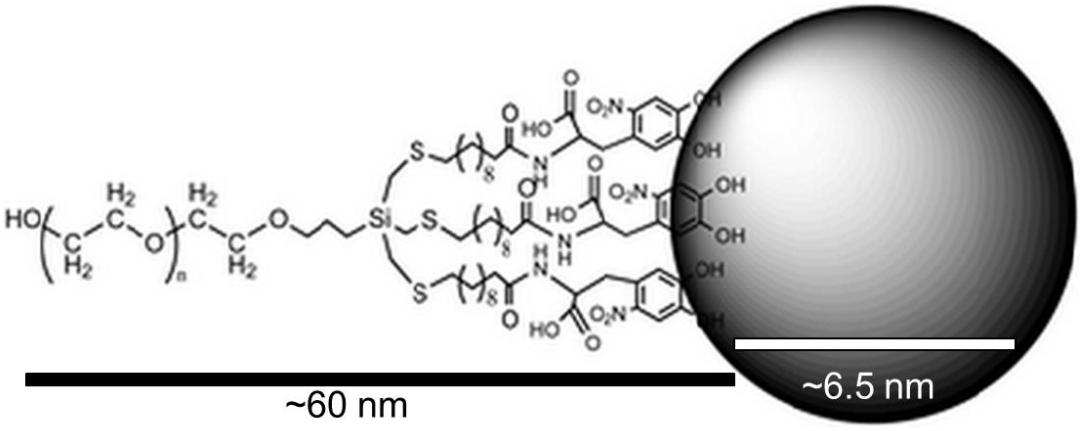

Figure 3. Schematic of the Fe_3O_4 NPs used in this study. Figure from Saville *et al.* 2012.

Amoebae Viability and Replication

Fe_3O_4 NPs are considered to be non-toxic in biological systems (21, 51). We found no significant effect on viability in amoebae after exposure to Fe_3O_4 NPs in either TSB or MHW (Table 2). Additionally, when amoebae were exposed to Fe_3O_4 NPs in MHW for 24, 48 or 72 hours and then transferred back into TSB, no differences in replication rate was seen between the control and exposed amoebae (Figure 4).

Table 2. Viabililty of *A. polyphaga* after exposure to NPs in growth medium or MHW.

Media	**Exposure time (h)**	**Control**		**Fe_3O_4 NPs**	
		% cysts	% live	% cysts	% live
TSB	24	-	97.6	-	97.7
TSB	48	-	97.7	-	97.4
MHW	24	45.8	21.8	58.7	17.1
MHW	48	45.0	6.4	64.7	2.0
MHW	72	52.1	1.9	50.8	7.7

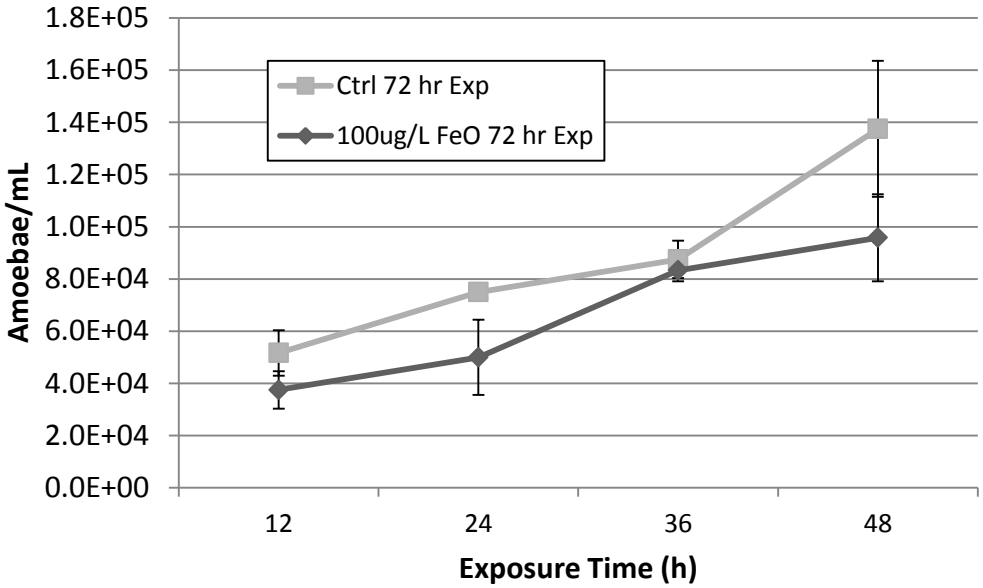

Figure 4. Replication of *A. polyphaga* in growth medium after 72 hour exposure to NPs in MHW.

Amoebae – *Legionella* Interaction Assays

Planktonic Bacteria Infection Assay

Planktonic, stationary phase *L. pneumophila* readily invade and replicate within amoebae (49). Infection assays using *A. polyphaga* and planktonic *L. pneumophila* were conducted to determine if NP exposure affected this interaction. Stationary-phase bacteria were added to pre-established monolayers of amoebae either alone, with NPs, or after an overnight incubation of bacteria with NPs. Incubation of bacteria with AuNPs has been shown to lead to adsorption and uptake of the NPs by bacteria, although this did not affect the ability of the bacteria to infect amoebae (20, 38). No differences in the uptake or replication of bacteria with or without exposure to Fe_3O_4 NPs were found (Figure 5). Uptake of the bacteria was consistent with or without NP exposure with all

samples exhibiting approximately 10^6 bacteria/well after 2 hour incubation. Replication across all the samples increased from approximately 10^6 bacteria/well to 10^8 bacteria/well after 48 hour incubation. Previous work has shown a reduction in amoebae grazing on *L. pneumophila* biofilms after AuNP exposure (38).

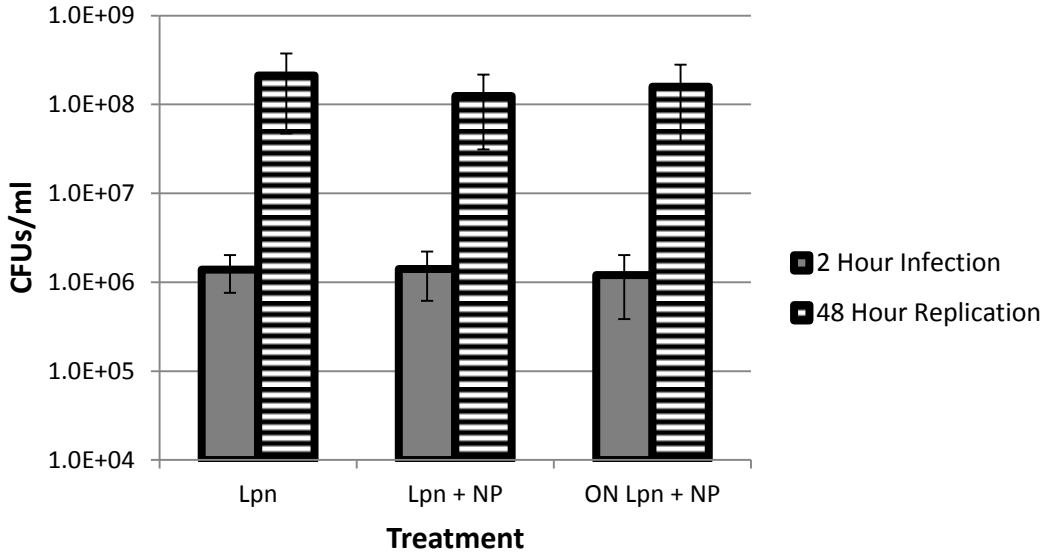

Figure 5. Analysis of *A. polyphaga* infection and replication ability by *L. pneumophila.* *A. polyphaga* infection with planktonic *L. pneumophila* without NPs (Lpn), after exposure to NPs simultaneously (Lpn + NP), or with previous concurrent planktonic incubation with NPs (ON Lpn + NP). No significant difference was seen in the infection and replication ability of the bacteria. Bars indicate mean±standard error (n=3).

Amoebae grazed equally well however on *L. pneumophila* biofilms exposed to Fe_3O_4 NPs as on unexposed biofilms (Figure 6). Significant reductions in surface area were observed after amoebae grazing in both controls and NP exposed biofilms. (p=0.004; p=0.007). Control biofilms demonstrated a 42% reduction in surface area after grazing while NP exposed biofilms were reduced by 46%.

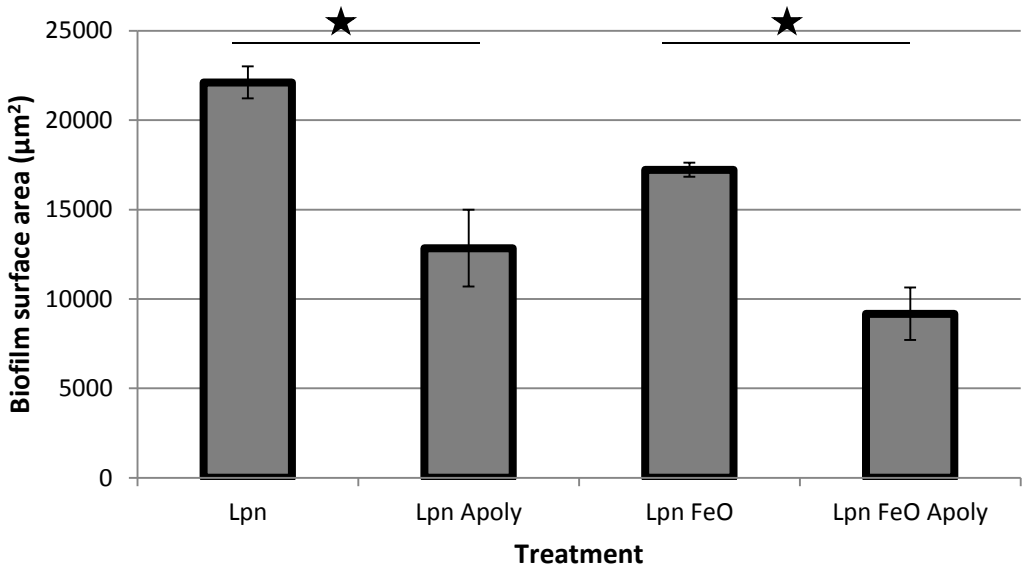

Figure 6. Analysis of *L. pneumophila* biofilm surface area after grazing by *A. polyphaga.* with and without exposure to 1µg/L Fe_3O_4 NPs. *Asterisks* indicate significant differences from respective controls according to ANOVA (p<0.05). Bars represent mean±standard error (n=5). *Lpn : L. pneumophila, Apoly: A. polyphaga, FeO NP:* iron oxide nanoparticle.

Next, amoebae survival was analyzed to determine if changes in bacterial virulence occurred after NP exposure. Amoebae grazing on control biofilms normally results in reduced amoebae survival due to lysis of the amoebae through replication of the bacteria. No significant difference was found in survival of amoebae from control versus treated biofilms (Figure 7). In control biofilms, amoebae numbers were reduced by 94.25% from the initial amount added; in treated biofilms, amoebae numbers were reduced by 90.25%.

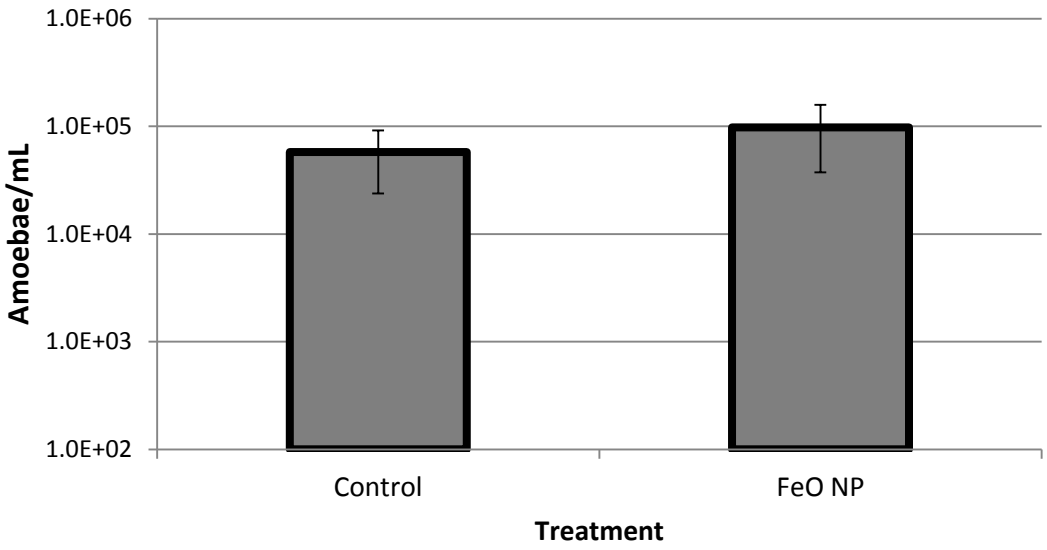

Figure 7. *A. polyphaga* survival after grazing on control or Fe_3O_4 NP exposed biofilms. Bars represent mean±standard deviation (*n*=5). *FeO NP:* iron oxide nanoparticle.

Analysis of Dispersed Biofilm

NPs have been shown to disrupt biofilms and induce biomass dispersal, making it important to understand the composition of biomass being released from the biofilm (20). Biomass released from *L. pneumophila* biofilms could result in greater exposure of the pathogen to humans. Bacterial cells released from biofilms as a result of NP exposure were measured as CFUs/mL. CFUs measure the amount of viable bacteria through a series of dilutions on agar plates. There was no significant difference found between the amount of viable bacteria released from biofilms after exposure to MHW alone or MHW with 100 μg/L Fe_3O_4 NPs, suggesting that the difference in biomass loss is due to dead cell infrastructure (Figure 8).

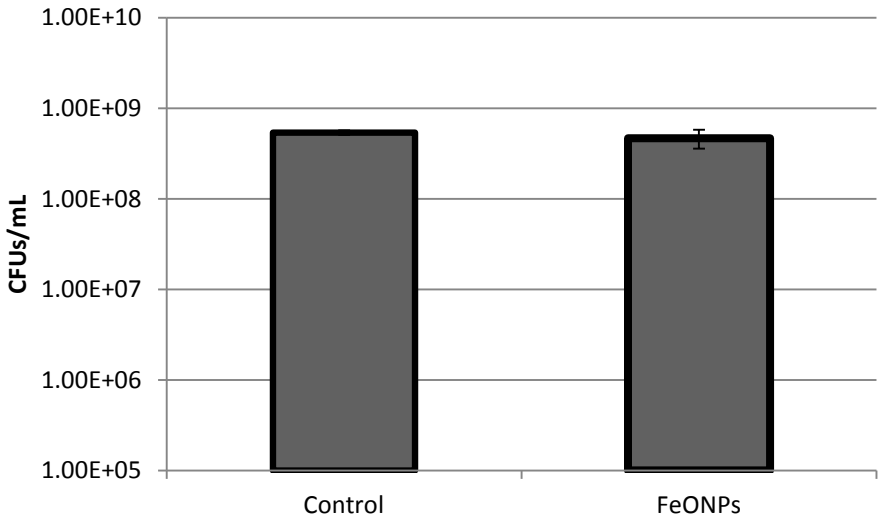

Figure 8. CFUs/mL of *L. pneumophila* biofilm supernatant after exposure to Fe_3O_4 NPs. Bars represent mean±standard deviation (*n*=3). *FeONP:* iron oxide nanoparticle.

Microscopy: Nanoparticle-Biofilm Interaction

CytoViva Hyperspectral Microscopy

The CytoViva hyperspectral imaging system showed integration of AuNPs and Fe_3O_4 NPs within the *L. pneumophila* biofilm (Figure 9). Spectral angle mapping (SAM) classification overlay matched several areas of interest in the treated biofilm to the spectral library file (SLF) generated from pure AuNPs or pure Fe_3O_4 NPs. No matches occurred in control biofilms (Figure 9a). Matched areas appear red in the NP exposed biofilms and show AuNPs embedded within the biofilm matrix as well as clustered around the edges of individual bacteria (Figure 9b). Matches showing clusters of particles embedded within the biofilm are seen in biofilms exposed to Fe_3O_4 NPs (Figure 9c).

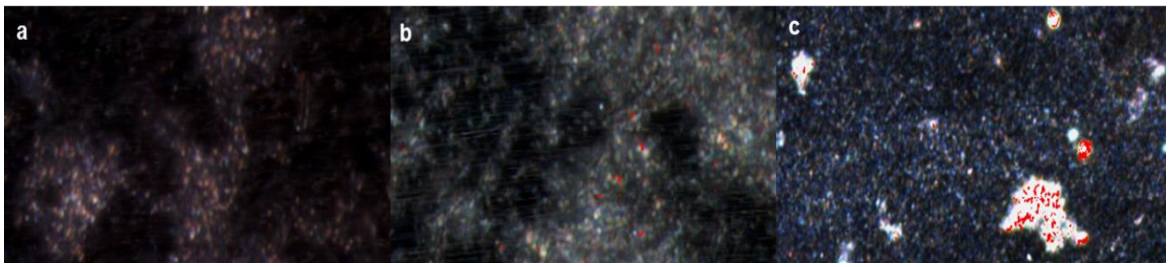

Figure 9. Hyperspectral SAM classification overlay images taken at 60X on a CytoViva hyperspectral microscope. a) Control *L. pneumophila* biofilm b) *L. pneumophila* biofilm treated with 100µg/L AuNPs c) *L. pneumophila* biofilm treated with 100µg/L Fe_3O_4 NPs. Red patches indicate a match with AuNP spectral library data. Scale bars cannot be accurately added to hyperspectral images.

Leica Ground State Depletion Microscopy with Cy5.5-Fe_3O_4 NPs

A Leica SR GSD 3D microscopy system was used to image the Fe_3O_4 NPs within the biofilm. GSD 3D images of Syto 11 stained control biofilms (green) showed expected morphology with a homogenous layer of bacteria (green) and no Cy5.5-Fe_3O_4 NPs signal (Figure 10a). Syto11 stains both intracellular and extracellular nucleic acids within the biofilm. Control biofilms demonstrate foci of likely chromosomal DNA staining as well as possible eDNA staining. Biofilms exposed to the Cy5.5-Fe_3O_4NPs show both the Syto11 stained DNA (green) and Cy5.5-Fe_3O_4 NPs (red) appearing at the edges of individual bacteria (Figure 10b). After exposure to the Cy5.5-Fe_3O_4 NPs, biofilms appear sparser with less connective staining suggesting the loss of overall biomass calculated in previous experiments (38). In standard biofilm-Cy.5.5-Fe_3O_4 NP interaction assays, biomass loss similar to that with the untagged Fe_3O_4 NPs occurred.

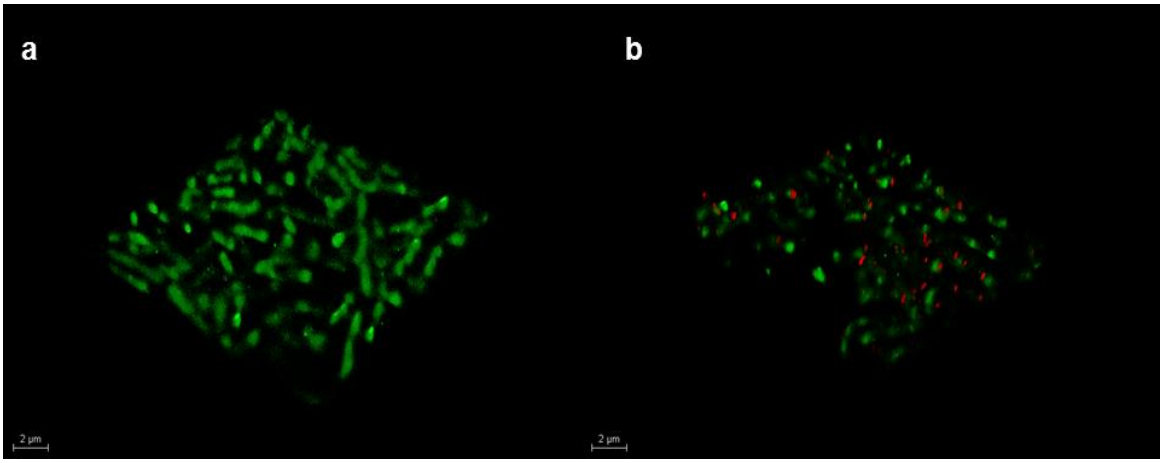

Figure 10. Leica SR GSD 3D images show Fe_3O_4 NPs embedded within biofilms. a) Control *L. pneumophila* biofilm b) *L. pneumophila* biofilm treated with 100µg/L Cy5.5 tagged Fe_3O_4 NPs.

AuNP-pDNA Binding Analysis

Citrate-capped AuNPs have been shown to tightly bind and stabilize DNA (35). We assessed binding between AuNPs and pDNA in MHW. AuNPs added to MHW demonstrated aggregation over time as measured by the increase in DLS diameter. Sizes shifted from an initial 20nm size in the stock solution to over 100nm in MHW. The ionic strength of MHW diminishes particle stability and the monodispersed state of citrate capped-AuNPs. Exposure to MHW alone decreased the colloidal stability and increased the aggregation state of the AuNPs (Figure 11, black lines). The addition of plasmid DNA (pDNA) exhibited a strong stabilizing effect on AuNPs, maintaining a consistent NP size of 20nm (Figure 11, blue lines). AuNPs were stabilized through the addition of pDNA in MHW almost instantly at 0 min. This stabilization effect continued after 30 min of exposure to pDNA. Samples of AuNPs plus pDNA incubated up to 72h showed no evidence of aggregation. The inherent stability of the Fe_3O_4 NPs prevents this type of analysis from being conducted.

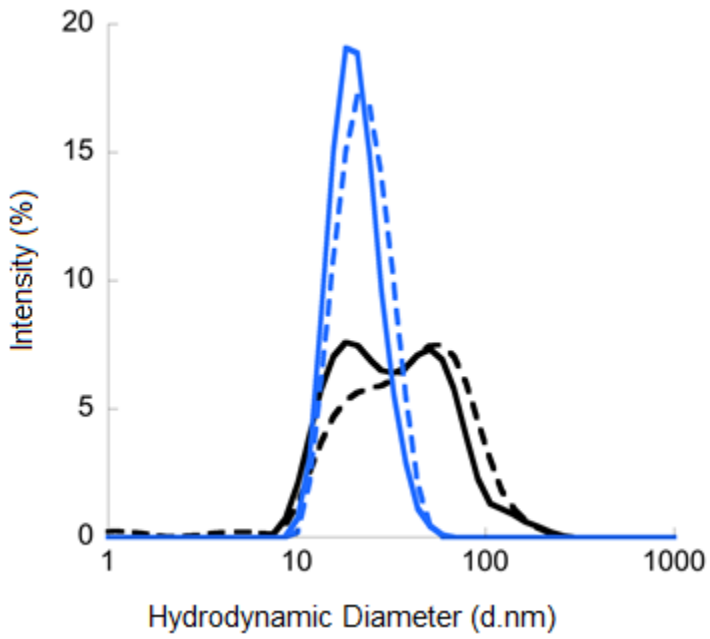

Figure 11. Time-course measurements of AuNP diameter (nm) s in MHW by DLS. Solid lines indicate t=0, dotted lines indicate t=30 min. Blue lines represent addition of plasmid DNA, black lines represent control (*n*=2).

Biofilm Interaction Analysis

eDNA is an important matrix component in many microbial biofilms but has not yet been shown to be present in *Legionella* biofilms. DNase treatment of mature *L. pneumophila* biofilms resulted in significant loss of bio-volume compared to untreated controls suggesting that eDNA is a major constituent of the EPS ($p=0.023$). Further analysis where biofilms were first exposed to either AuNPs or Fe_3O_4 NPs then treated with DNase however, were similar in biomass, roughness and thickness as biofilms treated only with NPs (Figure 12a). Biofilms first treated with DNase then followed by exposure to NPs also demonstrated similar bio-volumes, suggesting the two treatments were disrupting biofilm stability through similar or related mechanisms (Figure 12b).

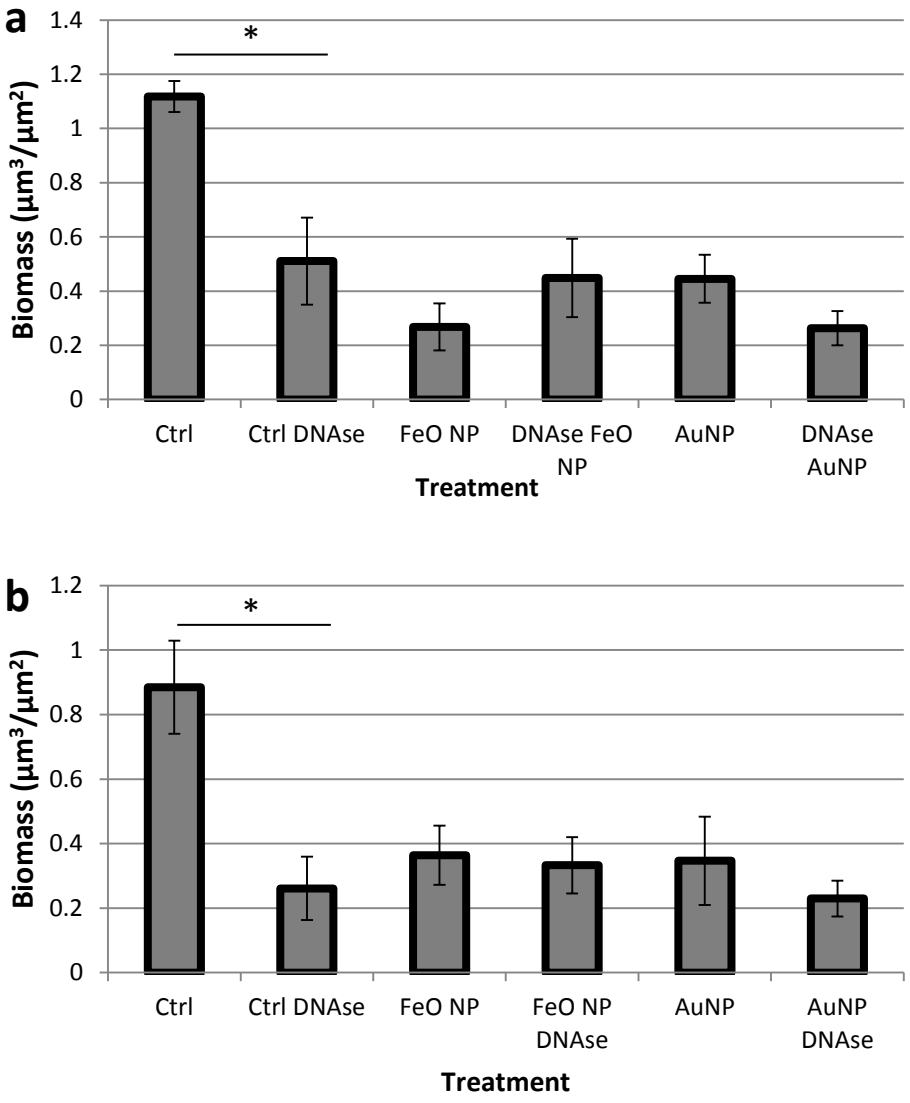

Figure 12. Biomass of *L. pneumophila* biofilms after DNase, Fe_3O_4 NPs or combined exposure. a) Biomass analysis using DNase first, followed by NPs in combined exposures. b) Biomass analysis using NP exposure first, following by DNase treatment in combined exposures. Asterisks indicate significant different from each respective control according to ANOVA (p<0.05). Bars represent mean±standard error (n=3). *Ctrl:* Control, *FeO NP*: iron oxide nanoparticle, *AuNP:* gold nanoparticle.

DISCUSSION

Microbial biofilms are an essential component of aquatic ecosystems. These highly organized, dynamic communities of bacteria are indispensable for biogeochemical cycling of carbon, nitrogen, sulfur, and oxygen (13). These biofilms also make up the base of the food web as they serve as a food source for protozoa. Disruption of biofilms and the processes associated with them could potentially have far-reaching impacts on entire ecosystems. The new threat of ecosystem contamination with engineered nanomaterials has not been fully investigated and the risks are largely unknown. NPs are found in a wide variety of consumer products, including sunscreens and cosmetics, which have the potential to enter into aquatic environments. Studies concerning the impact of engineered NPs on these ecosystems often focus on toxicity to fish, crustaceans, and other higher organisms. There is a paucity of research concerning the direct impact of NPs on microbial biofilms and the consequences of these interactions. A majority of the studies that have been conducted analyzing bacteria-NP interactions tend to focus on eradication of bacteria, often in industrial or medical settings (11, 15, 52). While it has been established that some NPs, such as AgNPs or CuONPs, exhibit antibacterial properties to planktonic bacteria, little research has been done to understand the effects of these NPs on bacteria within biofilms. Biofilms are the preferred niche of most bacteria in the environment and are the most likely reservoir in which contaminating NPs will be retained. Many studies have also focused on bacteria that may be unlikely to encounter NPs in aquatic environments; therefore it is important to consider an environmentally relevant microorganism when investigating NP-biofilm interactions (15). It is for this

reason that the ubiquitous freshwater biofilm-forming bacterium, *Legionella pneumophila*, was selected for this study. The rapid increase in integration of NPs into consumer products suggests that the risk of NP contamination on biofilms is a priority area for investigation.

Previously, we demonstrated that exposure of *L. pneumophila* biofilms to low concentrations of stable, discrete NPs induced dispersal events likely due to an increased vulnerability to flow forces (20, 21). 18 nm AuNPs at a concentration of 0.7 μg/L were found to induce dispersal of biomass. Similarly sized AuNPs at a concentration of 100 μg/L and 50 nm AuNPs did not induce dispersal events. It has been hypothesized that NP-biofilm interaction is largely governed by NP size. Larger NPs or aggregates of unstable NPs do not appear to interact with *L. pneumophila* biofilms in the same manner that discrete, smaller NPs do. Platinum (Pt) NPs and novel Fe_3O_4 NPs initiate biomass dispersal similarly to that seen with 18 nm AuNPs (21). This indicates that the ability of an NP to remain discrete within solution, rather than the core chemistry itself, plays a more important role in dictating that NP's ability to induce a dispersal event and interact with the biofilm. Several studies indicate that diffusion of NPs within the biofilm follows a similar size dependency to what we have previously demonstrated. A study using *Pseudomonas fluorescens* biofilms demonstrated that as particle size increases, diffusion of particles within the biofilm generally decreases (53). Another study confirmed that NP size, rather than surface charge or chemistry, had a greater impact on the ability of NPs to become embedded within *P. fluorescens* biofilms. Using functionalized silicon, gold, and titanium NPs, the study found that there was no significant difference in diffusion

coefficient between negatively and positively charged probes. In the same study, NPs larger than 10 nm were found to have a decreased diffusion coefficient compared to smaller NPs. NPs over 65 nm were completely excluded from biofilms altogether (54). The stability of NPs as they enter aquatic systems remains an important factor in determining their impact on these environments. The Fe_3O_4 NPs used in this study employ a novel surface polymer coating that allows them to remain highly discrete in a wide variety of media. Understanding how these super-stable NPs interact with biofilms on a molecular level as a discrete entity will further our ability to assess potential outcomes of environmental NP contamination.

Since stable NPs cause biomass dispersal it is important to analyze the composition of the biomass being lost from the biofilm. If live cells are a major component lost from *Legionella* biofilms upon NP exposure, this could indicate a potential public health hazard that could result in widespread dissemination of the pathogen. We found that biomass released from biofilms exposed to AuNPs or Fe_3O_4 NPs is composed of similar numbers of viable cells. This indicates that a larger percentage of dead cells are being released from biofilms exposed to NPs since more overall biomass, as quantified by microscopy, is released. Dead bacterial cells are a known component of biofilms and serve as a source of extracellular DNA within the biofilm matrix (30, 55). It is likely that disruption of a component in the EPS that is responsible for interaction with dead cells in the biofilm could preferentially cause the release of these cells after exposure to flow forces. Here we have shown evidence that novel Fe_3O_4 NPs and AuNPs become physically embedded in the EPS matrix of the biofilm. Deposition of both NPs

within the biofilm was observed using CytoViva microscopy. We know from previous studies that these NPs induce biomass dispersal similarly, and due to their location within the biofilm, we propose that the mechanism of action by these two NPs is similar or related.

Biofilm EPS is composed of proteins, extracellular DNA, and exopolysaccharides and is the glue that holds biofilms together (22, 30). While the general constituents of the biofilm are known, it still remains unclear the exact role each of these constituents play in the *Legionella* biofilm. Our previous data shows that a variety of NPs induce biomass dispersal of *L. pneumophila* biofilms likely through interactions with matrix components. NPs may help us elucidate how specific matrix components are important for stabilization of the biofilm. We hypothesize that these NPs are interacting with some component of the EPS, possibly extracellular DNA (eDNA), to disrupt the biofilm and induce dispersal. Molecular interaction between AuNPs and DNA has been characterized showing that DNA can tightly bind and stabilize citrate-capped AuNPs. (35). Recent research has delved into the diagnostic and therapeutic applications of DNA-modified NPs. Several recent studies have investigated the ability of DNA loading onto AuNP surfaces (56). In the current study, DLS was used to measure the hydrodynamic radius of AuNPs over time in the presence and absence of plasmid DNA (pDNA) in MHW. In MHW, which replicates environmental water conditions, AuNPs were shown to become unstable and quickly aggregate. Citrate-capped AuNPs, such as those used in this study, remain stable in UPW due to electrostatic repulsion as measured by zeta potential. The addition of pDNA to AuNPs in MHW leads to stabilization of these NPs, creating more

discrete and uniform particles over time. DNA adsorption to citrate-capped AuNPs has been shown to occur quickly, especially in high salt environments (35). This same interaction could not be measured for the Fe_3O_4 NPs, as these NPs are already highly discrete, non-aggregating particles, even in biological media (47). Fe_3O_4 NPs have a zeta potential close to zero indicating that steric hindrance is likely the mechanism of stabilization of the particles in solution rather than electrostatic repulsion. While potential binding of DNA to Fe_3O_4 NPs could not be shown through use of zeta potential measurements, other studies have indicated a potential interaction between DNA and polyethylene glycol (PEG). The Fe_3O_4 NPs used in this study have a small core of 7.4 nm as observed by transmission electron microscopy. A large PEG polymer complex is attached to the core increasing the overall hydrodynamic diameter. This large polymer is most likely what is truly interacting with the biofilms rather than the metallic core. Nucleotides, particularly guanine and thymine, have been shown to bind to PEG. Entire strands of DNA exhibit the phenomena of condensation in the presence of high PEG solutions. It has been suggested that PEG and DNA interact via hydrophobic and hydrophilic interactions to form DNA condensates (57). Thus, in our system it is possible that eDNA may be disrupted by the PEG polymer complex attached to the Fe_3O_4 NPs leading to biofilm destabilization. To determine if Fe_3O_4 NPs may be disrupting eDNA, we used advanced microscopy techniques along with Cy5.5-tagged Fe_3O_4 NPs to visualize the location of the labelled NP within the biofilm as well as differences in connective staining of the biofilm after NP exposure. We demonstrate here that biofilms exposed to Fe_3O_4 NPs exhibited less connective nucleic acid staining after treatment.

Biofilms were stained with Syto11, a dye that stains all nucleic acids within biofilm both extracellular and intracellular. We were able to observe less stain between bacteria after NP treatment indicating a loss of eDNA. We hypothesize that Fe_3O_4 NPs are likely binding eDNA similarly to what is seen between DNA and AuNPs.

eDNA has been shown to be essential for biofilm formation of several different species of bacteria (30-32, 34, 58). In particular, eDNA has been shown to be essential for biofilm formation and expansion in *Pseudomonas aeruginosa* biofilms. DNase I present in culture medium inhibited biofilm formation and prevented biofilm expansion (34). Using a similar experimental model, we found that mature *L. pneumophila* biofilms treated with DNase I in MHW resulted in a decrease in biomass similar to that of biofilms treated with AuNPs or Fe_3O_4 NPs alone. This phenomenon has led us to believe that perhaps AuNPs and Fe_3O_4 NPs are disrupting eDNA within the biofilm leading to overall biofilm disruption. To investigate if NPs and DNA were in fact working through a similar mechanism to destabilize biofilms, we exposed DNase I treated biofilms to NPs as well as exposing biofilms already treated with NPs to a subsequent DNase treatment. No significant changes to biomass, thickness, or roughness of the biofilm were observed in either of the secondary treatments. This result suggests that eDNA plays an important role in stabilization of *L. pneumophila* biofilms and that eDNA is also involved in NP-biofilm interactions. As previously stated, the role of eDNA in the *Legionella* biofilm has yet to be characterized. At this time, this is the first study to implicate eDNA as an important component necessary for stabilization of these biofilms. In addition to directly interacting with eDNA resulting in biofilm destabilization, it is possible that NPs could

interact with eDNA stabilizing proteins or connecting pili. eDNA has been found to facilitate twitching motility-mediated biofilm expansion and cell migration guided by eDNA (31). Type IV pili have been proposed to bind to eDNA to mediate biofilm expansion in *P. aeruginosa* biofilms (31). It is possible that the *L. pneumophila* type IV pili plays a similar role to the *P. aeruginosa* type IV pili in formation and organization of a maturing biofilm. The type IV pilus in *L. pneumophila* has been shown to be an important factor in biofilm colonization and formation (59). Further studies are needed to identify other potential factors in *L. pneumophila* early biofilm attachment and development. Identification of these factors will not only help us understand the *Legionella* biofilm better, but also help us understand the effect NPs may have on environmental microbial biofilms.

By characterizing NP interactions with important components of the EPS we can begin to understand the repercussions of these interactions on entire ecosystems. It is known that EPS matrix can play a role in dictating predator-prey interactions. Biofilm morphology in particular has been shown to be important in dictating the interaction of microbial biofilms with protozoan grazers. The formation of microcolonies by *P. aeruginosa* and *Serratia marsescens* biofilms has been shown to protect these communities from grazing by flagellate feeders (39, 60). However, in both cases, microcolony formation was not enough to protect the biofilm from surface feeders such as *A. polyphaga*. Filamentous and chain-like *S. marsescens* biofilm structures did contribute to grazing resistance from *A. polyphaga*, implying biofilm morphology plays a complex role in defining protozoan grazing preferences. Numerous factors play a role in

feeding preferences, including biofilm morphology and topography, motility of the grazer, and dissolved chemical cues (39, 60, 61). The model system used in this study between *L. pneumophila* and the amoeba *A. polyphaga* has been well-characterized. These amoebae serve as a host in which the bacteria can replicate and survive chemical treatments. *L. pneumophila* biofilms are grazed upon by amoeba leading to uptake of the bacteria. Once inside the amoeba, the bacteria replicate and lead to the lysis of these amoebae. Previously we showed that treatment of *L. pneumophila* biofilms with AuNPs altered the biofilm grazing ability of *A. polyphaga* (38). To investigate the mechanism behind this alteration, the same experiments were repeated utilizing Fe_3O_4 NPs. Interestingly, although Fe_3O_4 NPs also alter biofilm morphology similar to that seen with AuNPs, this did not result in changes to amoebae behavior. Biofilm biomass decreased similarly after *A. polyphaga* grazing in both control and Fe_3O_4 NP treated biofilms. Survival of amoebae was also similarly decreased between control and exposure biofilm conditions. This suggests that morphological change of the biofilm is not the only factor influencing grazing ability. Neither NP type resulted in direct toxicity to the bacteria or the amoebae, but AuNPs may elicit the production of dissolved chemical cues from the biofilm that alter the way in which amoebae sense the biofilm. Dissolved chemical cues have been shown to influence preferential feeding of protozoa on bacterial biofilms (61). The production of certain chemical signals such as amino acids has been shown to have inhibitory effects on feeding by ciliates (62). These chemical cues could potentially deter amoeba from grazing on the biofilm in our model system. To determine if NP treatment were perhaps negatively affecting the amoebae themselves, several experiments were

conducted to rule out this possibility. Viability over time was assessed in both growth medium and MHW with no significant effects seen due to Fe_3O_4 NP exposure. No significant change in replication ability was observed either, thus eliminating the possibility that Fe_3O_4 NPs are affecting amoebae alone. Similar results were also seen when these experiments were conducted using AuNPs (38). Planktonic interactions between amoebae and *L. pneumophila* were also not affected suggesting that both AuNPs and Fe_3O_4 NPs do not alter virulence of the bacteria in regards to invasion and replication ability. *L. pneumophila* was able to efficiently invade and replicate intracellularly in controls, after planktonic incubation with Fe_3O_4 NPs, and during simultaneous addition of Fe_3O_4 NPs, similar to results seen in treatments with AuNPs (38). More research is needed to determine what environmental cues could be altered by AuNPs to alter trophic interactions between bacteria and amoebae. Here we show that NP chemistry is important in determining how NP contamination impacts ecosystems.

Biofilms are an often overlooked essential part of aquatic ecosystems. As NP use increases, risk for contamination of aquatic systems also increases making it essential to understand their effects at all levels, including the very small. Very few studies have explored how NP contamination will affect microbes in the environment and more research is needed to understand the consequences of NP contamination. NPs are shown to cause biomass dispersal and in some cases, disrupt trophic interactions. While disruption of these interactions may not be true for all NP chemistries, the current lack of understanding of the molecular mechanisms behind NP-biofilm interactions does not allow for generalizations. A wider variety of surface and core chemistries of NPs may

have a myriad of different effects on bacteria. It is also important to note the increased use of highly stable NPs, particularly in the medical therapeutics and diagnostics field. As these NPs are excreted into water systems and eventually enter aquatic environments, highly stable NPs will behave differently than other NPs that may aggregate or precipitate in these environments. The understanding of discrete NPs on microbes, especially environmentally associated biofilms, will become even more important. Understanding the direct molecular effects and resulting system alterations will increase our ability to predict the effects on ecosystems and develop preventive measures to protect the environment.

WORKS CITED

1. **Becker S.** 2013. Nanotechnology in the marketplace: how the nanotechnology industry views risk. J. Nanopart. Res. **15:**. doi: 10.1007/s11051-013-1426-7.

2. **Handy, RD, Owen, R, Valsami-Jones, E.** 2008. The ecotoxicology of nanoparticles and nanomaterials: current status, knowledge gaps, challenges, and future needs. Ecotoxicology. **17:**315-325. doi: 10.1007/s10646-008-0206-0.

3. **Moore, MN.** 2006. Do nanoparticles present ecotoxicological risks for the health of the aquatic environment? Env. Int. **32:**967-976. doi: 10.1016/j.envint.2006.06.014.

4. **Bashaw, J.** 2012. Hazardous Substances, CERCLA, and Nanoparticles - Can the Three be Reconciled? Dose Response. **10:**397-404. doi: 10.2203/dose-response.10-021.Bashaw.

5. **Bondarenko, O, Juganson, K, Ivask, A, Kasemets, K, Mortimer, M, Kahru, A.** 2013. Toxicity of Ag, CuO and ZnO nanoparticles to selected environmentally relevant test organisms and mammalian cells in vitro: a critical review. Arch Toxicol. **87:**1181-1200. doi: 10.1007/s00204-013-1079-4.

6. **Aiken, GR, Hsu-Kim, H, Ryan, JN.** 2011. Influence of dissolved organic matter on the environmental fate of metals, nanoparticles, and colloids. Environ. Sci. Technol. **45:**3196-3201. doi: 10.1021/es103992s.

7. **Klaine, SJ, Alvarez, PJJ, Batley, GE, Fernandes, TF, Handy, RD, Lyon, DY, Mahendra, S, McLaughlin, MJ, Lead, JR.** 2009. Nanomaterials in the environment: behavior, fate, bioavailability, and effects. Environ. Toxicol. **27:**1825-1851.

8. **Pakrashi, S, Dalai, S, Ritika, B, Sneha, N, Chandrasekaran, AM.** 2012. A temporal study on fate of Al(2)O(3) nanoparticles in a fresh water microcosm at environmentally relevant low concentrations. Ecotox. Environ. Safe. **84:**70-77. doi: 10.1016/j.ecoenv.2012.06.015.

9. **Baun, A, Hartmann, NB, Grieger, K, Kusk, KO.** 2008. Ecotoxicity of engineered nanoparticles to aquatic invertebrates: a brief review and recommendations for future toxicity testing. Ecotoxicology. **17:**387-395. doi: 10.1007/s10646-008-0208-y.

10. **Mortimer, M, Kasemets, K, Kahru, A.** 2010. Toxicity of ZnO and CuO nanoparticles to ciliated protozoa *Tetrahymena thermophila*. Toxicology. **269:**182-189. doi: 10.1016/j.tox.2009.07.007.

11. **Marambio-Jones, C, Hoek, EMV.** 2010. A review of the antibacterial effects of silver nanomaterials and potential implications for human health and the environment. J. Nanopart. Res. **12:**1531-1551. doi: 10.1007/s11051-010-9900-y.

12. **Ud-Daula, A, Pfister, G, Schramm, KW.** 2013. Method for toxicity test of titanium dioxide nanoparticles in ciliate protozoan Tetrahymena. J. Environ. Sci. Health. **48:**1343-1348. doi: 10.1080/10934529.2013.781878.

13. **Paerl, HW, Pinckney, JL.** 1996. A Mini-Review of Microbial Consortia: Their Roles in Aquatic Production and Biogeochemical Cycling. Microb. Ecol. **31:**225-247.

14. **Maurer-Jones, MA, Gunsolas, IL, Murphy, CJ, Haynes, CL.** 2013. Toxicity of Engineered Nanoparticles in the Environment. Anal. Chem. **85:**3036-3049. doi: 10.1021/ac303636s.

15. **Masurkar, SA, Chaudhari, PR, Shidore, VB, Kamble, SP.** 2013. Effect of biologically synthesised silver nanoparticles on Staphylococcus aureus biofilm quenching and prevention of biofilm formation. IET Nanobiotechnol. **6:**110-114. doi: 10.1049/iet-nbt.2011.0061.

16. **Xu, C, Sun, S.** 2013. New forms of superparamagnetic nanoparticles for biomedical applications. Adv. Drug Deliver. Rev. **65:**732-243.

17. **Huang, Z, Zheng, X, Yan, D, Yin, G, Liao, X, Kang, Y, Yao, Y, Huang D., Hao, B.** 2008. Toxicological effect of ZnO nanoparticles based on bacteria. Langmuir. **24:**4140-4144. doi: 10.1021/la7035949.

18. **Suresh, AK, Pelletier, DA, Doktycz, MJ.** 2013. Relating nanomaterial properties and microbial toxicity. Nanoscale. **5:**463-474. doi: 10.1039/C2NR32447D.

19. **Suresh, AK, Pelletier, DA, Wang, W, Broich, ML, Moon, JW, Gu, B, Allison, DP, Joy, DC, Phelps, TJ, Doktycz, MJ.** 2011. Biofabrication of discrete spherical gold nanoparticles using the metal-reducing bacterium *Shewanella oneidensis*. Acta. Biomater. **7:**2148-2152. doi: 10.1016/j.actbio.2011.01.023.

20. **Stojak, A, Raftery, T, Klaine, S, McNealy, T.** 2012. Morphological responses of *Legionella pneumophila* biofilm to nanoparticle exposure. Nanotoxicology. **5:**730-742. doi: 10.3109/17435390.2010.550696.

21. **Raftery, T, Kerscher, P, Hart, A, Saville, SA, Qi, B, Kitchens, CL, Mefford, OT, McNealy, T.** 2013. Discrete nanoparticles induce loss of *Legionella pneumophila* biofilms from surfaces. Nanotoxicology. . doi: doi:10.3109/17435390.2013.79653.

22. **Flemming, HC, Wingender, J.** 2010. The Biofilm Matrix. Nat. Rev. Microbiol. **8:**623-633. doi: 10.1038/nrmicro2415.

23. **Gao, L, Giglio, KM, Sondermann, H, Travis, AJ.** 2014. Ferromagnetic nanoparticles with peroxidase-like activity enhance the cleavage of biological macromolecules for biofilm elimination. Nanoscale. . doi: 10.10139/C3NR05422E.

24. **Seil, JT, Webster, TJ.** 2012. Antimicrobial appliations of nanotechnology: methods and literature. Int. J. Nanomedicine. **7:**2767-2781. doi: 10.2147/IJN.S24805.

25. **Markowska, K, Grudniak, AM, Wolska, KI.** 2013. Silver nanoparticles as an alternative strategy against bacterial biofilms. Acta. Biochim. Pol. **60:**523-530.

26. **Jiang, X, Wang, X, Tong, M, Kim, H.** 2013. Initial transport and retention behaviors of ZnO nanoparticles in quartz sand porous media coated with*Escherichia coli*biofilm. Environ. Pollut. **174:**38-49.

27. **Battin, TJ, Kammer, FVD, Weilhartner, A, Ottofuelling, S, Hofmann, T.** 2009. Nanostructured TiO(2): transport, behavior and effects on aquatic microbial communities under environmental conditions. Environ. Sci. Technol. **43:**8098-8104. doi: 10.1021/es9017046.

28. **Xiao, Y, Wiesner, MR.** 2013. Transport and Retention of Selected Engineered Nanoparticles by Porous Media in the Presence of a Biofilm. Environ. Sci. Technol. **47:**2246-2253. doi: 10.1021/es304501n.

29. **Fabrega, J, Renshaw, JC, Lead, JR.** 2009. Interactions of Silver Nanoparticles with *Pseudomonas putida* biofilms. Environ. Sci. Technol. **43:**9004-9009. doi: 10.1021/es901706j.

30. **Fleming, H, Neu, TR, Wozniak, DJ.** 2007. The EPS Matrix: The "House of Biofilm Cells". J. Bacteriol. **189:**7945-7947. doi: 10.1128/JB.00858-07.

31. **Gloag, ES, Turnbull, L, Huang, A, Vallotton, P, Wang, H, Nolan, LM, Mililli, L, Hunt, C, Lu, J, Osvath, SR, Monahan, LG, Cavaliere, R, Charles, IG, Wand, MP, Gee, ML, Prabhakar, R, Whitchurch, CB.** 2013. Self-organization of bacterial biofilms is facilitated by extracellular DNA. P. Natl. Acad. Sci. USA. **110:**11541-11546.

32. **Lappann, M, Claus, H, Van Alen, T, Harmsen, M, Elias, J, Molin, S, Vogel, U.** 2010. A dual role of extracellular DNA during biofilm formation of Neisseria meningitidis. Mol. Microbiol. **75:**1355-1371. doi: 10.1111/j.1365-2958.2010.07054.x.

33. **Harmsen, M, Lappann, M, Knochel, S, Molin, S.** 2010. Role of Extracellular DNA during biofilm formation by*Listeria monocytogenes*. Appl. Environ. Micro. **76:**2271-2279. doi: 10.1128/AEM.02361-09.

34. **Whitchurch, CB, Tolker-Nielsen, T, Ragas, PC, Mattick, JS.** 2002. Extracellular DNA Required for Bacterial Biofilm Formation. Science. **295:**1487. doi: 10.1126/science.295.5559.1487.

35. **Zhang, X, Servos, MR, Liu, J.** 2012. Surface Science of DNA Adsorption onto Citrate-Capped Gold Nanoparticles. Langmuir. **28:**3896-3902. doi: 10.1021/la205036p.

36. **Werlin, R, Priester, JH, Mielke, RE, Kramer, S, Jackson, S, Stoimenov, PK, Stucky, GD, Cherr, GN, Orias, E, Holden, PA.** 2011. Biomagnification of cadmium selenide quantum dots in a simple experimental microbial food chain. Nat. Nanotechnol. **6:**65-71. doi: 10.1038/nnano.2010.251.

37. **Madsen, EL, Sinclair, JL, Ghiorse, WC.** 1991. In situ biodegredation: microbiological patterns in a contaminated aquifer. Science. **252:**830-833.

38. **Raftery, TD, Lindler, H, McNealy, TL.** 2013. Altered Host Cell–Bacteria Interaction due to Nanoparticle Interaction with a Bacterial Biofilm - Springer. Microb. Ecol. **65:**496-503.

39. **Matz C, KS.** 2005. Off the hook - how bacteria survive protozoan grazing. Trends Microbiol. **13:**302-307.

40. **Declerck, P.** 2010. Biofilms: the environmental playground of *Legionella pneumophila*. Env. Microbiol. **12:**557-566. doi: 10.1111/j.1462-2920.02025.x.

41. **Bigot, R, Bertaux, J, Frere, J, Berjeaud, JM.** 2013. Intra-amoeba multiplication induces chemotaxis and biofilm colonization and formation for Legionella. PLoS ONE. **8:**. doi: 10.1371/journal.pone.0077875.

42. **Abdel-Nour, M, Duncan, C, Prashar, A, Rao, C, Ginevra, C, Jarraud, S, Low, DE, Ensminger, AW, Terebiznik, MR, Guyard, C.** 2014. The *Legionella pneumophila* Collagen-Like Protein Mediates Sedimentation, Autoaggregation, and Pathogen-Phagocyte Interactions. Appl. Environ. Microbiol. **80:**1441-1454. doi: 10.1128/AEM.03254-13.

43. **Duncan, C, Prashar, A, So, J, Tang, P, Low, DE, Terebiznik, M, Guyard, C.** 2011. Lcl of *Legionella pneumophila* is an immunogenic GAG binding adhesin that promotes interactions with lung epithelial cells and plays a crucial role in biofilm formation. Infect. Immun. **79:**2168-2181. doi: 10.1128/IAI.01304-10.

44. **Abdel-Nour, M, Duncan, C, Low, DE, Guyard, C.** 2013. Biofilms: The Stronghold of *Legionella pneumophila*. Int. J. Mol. Sci. **14:**21660-21675. doi: 10.3390/ijms141121660.

45. **Liu, Z, Lin, YE, Hwang, CC, Vidic, RD, Yu, VL.** 2006. Effect of flow regimes on the presence of *Legionella* within the biofilm of a model plumbing system. J. Appl. Microbiol. **101:**437-442. doi: 10.1111/j.1365-2672.2006.02970.x.

46. **Gole, A, Murphy, CJ.** 2004. Seed-mediated synthesis of gold nano-rods: role of size and nature of the seed. Chem. Mater. **16:**3633-3640. doi: 10.1021/cm0492336.

47. **Saville, ST, Stone, RC, Qi, B, Mefford, OT.** 2012. Investigation of the stability of magnetite nanoparticles functionalized with catechol based ligands in biological media. J. Mater. Chem. **22:**24909-24917. doi: 10.1039/C2JM34902G.

48. **Na, HB, Palui, G, Rosenberg, JT, Ji, X, Grant, HC, Mattoussi, H.** 2012. Multidentate Catechol-Based Polyethylene Glycol Oligomers Provide Enhanced Stability and Biocompatibility to Iron Oxide Nanoparticles. ACS Nano. **6:**389-399.

49. **McNealy T.L., Forsbach-Birk V., Shi C., Marre R.** 2005. The Hfq homologue in *Legionella pneumophila* demonstrates regulation by LetA and RpoS and interacts with the global regulator CsrA. J. Bacteriol. **187:**1527-1532. doi: 10.1128/JB.187.4.1527-1532.2005.

50. **Heydorn, A, Nielsen, AT, Hentzer, M, Sternberg, C, Giskov, M, Ersboll, BK, Molin, S.** 2000. Quantification of biofilm structures by the novel computer program COMSTAT. Microbiology. **146:**2395-2407.

51. **Hafeli, UO, Riffle, JS, Harris-Shekhawat, L, Carmichael-Baranauskas, A, Mark, F, Dailey, JP, Bardenstein, D.** 2009. Cell Uptake and *in Vitro* Toxicity of Magnetic Nanoparticles Suitable for Drug Delivery. Mol. Pharm. **6:**1417-1428. doi: 10.1021/mp900083m.

52. **Hannah, W, Thompson, PB.** 2008. Nanotechnology, risk and the environment: a review. J. Environ. Monit. **10:**291-300. doi: 10.1039/b718127m.

53. **Peulen, TO, Wilkinson, K.** 2011. Diffusion of Nanoparticles in a Biofilm. Environ. Sci. Technol. **45:**3367-3373. doi: 10.1021/es103450g.

54. **Golmohamadi, M, Clark, RJ, Veinot, J, Wilkinson, K.** 2012. The role of charge on the diffusion of solutes and nanoparticles (silicon nanocrystals, nTiO(2), nAu) in a biofilm. Envir. Chem. **10:**34-41. doi: 10.1071/EN12106.

55. **Webb, JS, Thompson, LS, James, S, Charlton, T, Tolker-Nielsen, T, Koch, B, Givskov, M, Kjelleberg, S.** 2003. Cell Death in *Pseudomonas aeruginosa* Biofilm Developmen. J. Bacteriol. **185:**4585-4592. doi: 10.1128/JB.185.15.4585-4592.2003.

56. **Hurst, SJ, Lytton-Jean, A, Mirkin, CA.** 2006. Maximizing DNA Loading on a Range of Gold Nanoparticle Sizes. Anal. Chem. **78:**8313-8318. doi: 10.1021/ac0613582.

57. **Froehlich, E, Mandeville, JS, Arnold, D, Kreplak, L, Tajmir-Riahi, HA.** 2011. PEG and mPEG-Anthracene Induce DNA Condensation and Particle Formation. J. Phys. Chem. **115:**9873-9879. doi: dx.doi.org/10.1021/jp205079u.

58. **Ma, L, Conover, M, Lu, H, Parsek, MR, Bayles, K, Wozniak, DJ.** 2009. Assembly and Development of the *Pseudomonas aeruginosa* Biofilm Matrix. Plos Pathog. **5:**. doi: 10.1371/journal.ppat.1000354.

59. **Lucas, CE, Brown, E, Fields, BS.** 2006. Type IV pili and type II secretion play a limited role in *Legionella pneumophila* biofilm colonization and retention. Microbiology. **152:**3569-3573. doi: 10.1099/mic.0.2006/000497-0.

60. **Queck, S, Weitere, M, Moreno, AM, Rice, SA, Kjelleberg, S.** 2006. The role of quorum sensing mediated developmental traits in the resistance of *Serratia marcescens* biofilms against protozoan grazing. Environ. Microbiol. **8:**1017-1025. doi: 10.1111/j.1462-2920.2006.00993.x.

61. **Dopheide, A, Lear, G, Stott, R, Lewis, G.** 2012. Preferential Feeding by the Ciliates Chilodonella and Tetrahymena spp. and Effects of These Protozoa on Bacterial Biofilm Structure and Composition. Appl. Environ. Microb. **77:**4564-4572.

62. **Strom, SL, Wolfe, GV, Bright, KJ.** 2007. Responses of marine planktonic protists to amino acids: feeding inhibition and swimming behavior in the ciliate *Favella* sp. Aquat. Microb. Ecol. **47:**107-121.